Thermal instability of a compound resonator

Ivan S. Grudinin and Kerry J. Vahala

California Institute of Technology, 1200 E. California blvd, Pasadena, CA 91125, USA
Grudinin@caltech.edu

Abstract: We investigate the thermal and Kerr nonlinearity in a system of two optically-coupled silica microtoroid resonators experimentally and theoretically. A model for two coupled oscillators describing nonlinear resonance curves is developed. Stability of the static solutions is analyzed. It is shown that thermal nonlinearity is responsible for driving the eigenfrequencies of the two resonators apart, making the normal modes of the system unstable as the pump power grows. The red-detuned normal mode becomes unstable for certain pumping powers.

OCIS codes: (190.1450) Bistability; (230.5750) Resonators.

References and links

1. V. S. Ilchenko, M. L. Gorodetsky, and S. P. Vyatchanin, "Coupling and tunability of optical whispering-gallery modes: a basis for coordinate meter," Opt. Commun. **107**(1-2), 41–48 (1994).
2. T. Mukaiyama, K. Takeda, H. Miyazaki, Y. Jimba, and M. Kuwata-Gonokami, "Tight-binding photonic molecule modes of resonant bispheres," Phys. Rev. Lett. **82**(23), 4623–4626 (1999).
3. A. A. Savchenkov, V. S. Ilchenko, T. Handley, and L. Maleki, "Second-order filter response with series-coupled silica microresonators," IEEE Photon. Technol. Lett. **15**(4), 543–544 (2003).
4. A. A. Savchenkov, V. S. Ilchenko, A. B. Matsko, and L. Maleki, "High-order tunable filters based on a chain of coupled crystalline whispering gallery-mode resonators," IEEE Photon. Technol. Lett. **17**(1), 136–138 (2005).
5. D. D. Smith, H. Chang, K. A. Fuller, A. T. Rosenberger, and R. W. Boyd, "Coupled-resonator-induced transparency," Phys. Rev. A **69**(6), 063804 (2004).
6. A. Naweed, G. Farca, S. I. Shopova, and A. T. Rosenberger, "Induced transparency and absorption in coupled whispering-gallery microresonators," Phys. Rev. A **71**(4), 043804 (2005).
7. D. D. Smith, and H. Chang, "Coherence phenomena in coupled optical resonators," J. Mod. Opt. **51**, 2503–2513 (2004).
8. B. Möller, U. Woggon, and M. V. Artemyev, "Photons in coupled microsphere resonators," J. Opt. A **8**, S113–S121 (2006).
9. A. V. Kanaev, V. N. Astratov, and W. Cai, "Optical coupling at a distance between detuned spherical cavities," Appl. Phys. Lett. **88**(11), 111111 (2006).
10. A. Mazzei, S. Götzinger, Lde. S. Menezes, G. Zumofen, O. Benson, and V. Sandoghdar, "Controlled coupling of counterpropagating whispering-gallery modes by a single Rayleigh scatterer: a classical problem in a quantum optical light," Phys. Rev. Lett. **99**(17), 173603 (2007).
11. M. Benyoucef, S. Kiravittaya, Y. F. Mei, A. Rastelli, and O. G. Schmidt, "Strongly coupled semiconductor microcavities: A route to couple artificial atoms over micrometric distances," Phys. Rev. B **77**(3), 035108 (2008).
12. A. E. Fomin, M. L. Gorodetsky, I. S. Grudinin, and V. S. Ilchenko, "Nonstationary nonlinear effects in optical microspheres," J. Opt. Soc. Am. B **22**(2), 459–465 (2005).
13. V. S. Il'chenko, and M. L. Gorodetskii, "Thermal nonlinear effects in optical whispering gallery microresonators," Laser Phys. **2**, 1004–1009 (1992).
14. D. K. Armani, T. J. Kippenberg, S. M. Spillane, and K. J. Vahala, "Ultra-high-Q toroid microcavity on a chip," Nature **421**(6926), 925–928 (2003).
15. V. B. Braginsky, M. L. Gorodetsky, and V. S. Ilchenko, "Quality-factor and nonlinear properties of optical whispering-gallery modes," Phys. Lett. A **137**(7-8), 393–397 (1989).

1. Introduction

Systems of two or more coupled whispering gallery mode (WGM) resonators have attracted considerable interest as the number of potential applications grows. It was shown that highly sensitive displacement sensing is possible with a pair of coupled silica microspheres [1]. Tight binding manipulation of light within contacting micrometer-scaled spheres having matching WGM frequencies has also been shown [2]. Second [3] and third [4] order optical filters were demonstrated using coupled silica and crystalline resonators. Moreover, the response of coupled optical resonators was pointed out to be physically similar to electromagnetically

#113430 - $15.00 USD Received 29 Jun 2009; revised 22 Jul 2009; accepted 22 Jul 2009; published 29 Jul 2009

induced transparency [5,6]; and along these lines coupled resonator systems were shown to be physically analogous to a two level atom with a number of effects predicted based on this analogy [7]. Coupled modes of microsphere resonators were also explored as building blocks for coupled-resonator optical waveguides (CROWs) [8,9] and have been studied in other contexts [10]. Modes in "photonic molecules" were proposed as a means to coherently transfer excitation between resonant quantum dots placed in different cavities [11]. Generally, the tunability of partial modes of a coupled resonator system through the optical coupling constant represents an important way of engineering the optical spectrum that can facilitate new applications of this configuration.

However, the unique combination of small mode volume and high optical Q factor of WGM resonators also leads to low thresholds for nonlinear effects. Heating of the material increases the refractive index, and combined with thermal expansion, shifts the cavity eigenfrequency. Furthermore, the optical Kerr effect also changes the refractive index. The question of how these mechanisms affect the response of a system of two coupled resonators is not a trivial one. Here, we present a model describing this response and show that the static solutions of this system can be very complex and sensitive to input parameters. We analyze the thermal and Kerr nonlinear effects in a system of two optically-coupled WGM resonators for the first time, showing that the thermal effect shifts the eigenfrequencies of the resonators such that the normal mode configuration becomes unstable for pumping at certain wavelengths. For example, the frequency of one of the resonators can be displaced far enough such that it effectively behaves as a single resonator. Several regimes are possible depending on the optical Q factors and dimensions of each resonator. These phenomena make the red partial supermode unstable at certain optical powers, which is an important limitation in future experiments.

2. Nonlinearity in the coupled whispering gallery mode resonators

We consider two WGM microtoroids brought together so that the WG modes are coupled via the evanescent field in a small gap between the toroids, as shown in Fig. 1. A tapered fiber coupler is used to deliver optical power to one of the resonators.

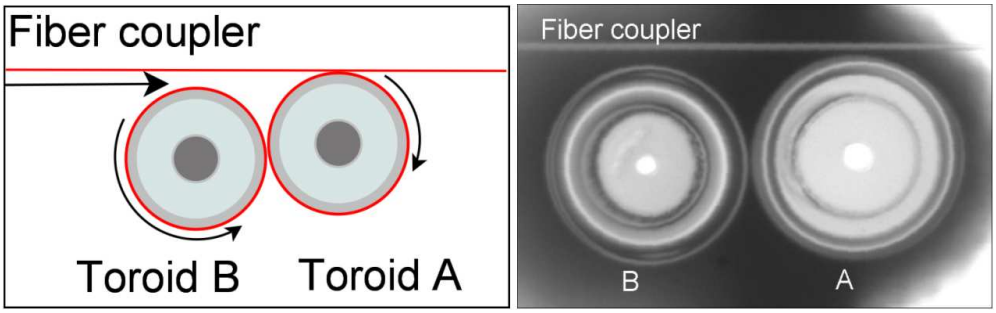

Fig. 1. Schematic and a photograph of the typical coupled toroid system.

We describe the electric field in the WGMs using the rotating wave approximation:

$$\vec{E}(\vec{r},t) = a(t)\vec{E}_0(\vec{r})e^{i\omega t}. \quad (1)$$

Here the distribution of the field in a specific WG mode of a resonator is normalized such that

$$\int \left|\vec{E_0}\right|^2 d\vec{r} = 1. \quad (2)$$

By analogy with the equations analyzed in [12] we introduce the equations describing the dynamics of the electric field slowly varying amplitudes ***a*** and ***b*** in resonator A and B with a coupling rate *k* in cgs units as

#113430 - $15.00 USD Received 29 Jun 2009; revised 22 Jul 2009; accepted 22 Jul 2009; published 29 Jul 2009

$$\begin{cases} \dot{a} + a(\gamma_a + i[\omega - \omega_a + \mu_a |a|^2 + \omega_a \beta_a \theta_a]) = iF + ikb \\ \dot{b} + b(\gamma_b + i[\omega - \omega_b + \mu_b |b|^2 + \omega_b \beta_b \theta_b]) = ika \\ \dot{\theta}_a + \delta_\theta^a \theta_a = \dfrac{\nu_a \delta_\theta^a}{\omega_a \beta_a} |a|^2 \\ \dot{\theta}_b + \delta_\theta^b \theta_b = \dfrac{\nu_b \delta_\theta^b}{\omega_b \beta_b} |b|^2 \end{cases} . \quad (3)$$

Here subscripts "*a*" and "*b*" denote the parameters of the corresponding resonators and $\dot{a} = \frac{da}{dt}$. Each toroid is characterized by its own major radius *R*, minor radius *r*, eigenfrequency ω, optical quality factor Q, and WG mode volume *V*. Here $\theta = \int (T - T_0) \left| \vec{E}_0(\vec{r}) \right|^2 \overrightarrow{dr}$ is the average heating over the volume of the WG mode. The parameter $\gamma = \frac{\omega}{2Q}$ is the optical loss rate. The generalized "force" created by the optical pump is $F = \sqrt{\frac{2\pi\omega_a W}{n^2 V_a Q_a}}$, where *W* is the pump laser power measured in *erg/s*. The parameters $\mu = \frac{2\pi\omega\chi^{(3)}}{n^2}$ and $\nu = \frac{\omega\beta n\alpha c}{4\pi C\rho\delta_\theta}$ define the resonator frequency shift due to the Kerr effect and thermal effect correspondingly. Here $\delta_\theta = D/b^2$, $D = k/(\rho C)$ is thermal diffusion coefficient (*k* - thermal conductivity), $b_a \simeq 0.84R\, l^{-2/3}$ is a half thickness of the WG mode in the radial direction, and *l* is the WGM azimuthal index (approximately equal to $2\pi Rn/\lambda$). $\beta = \frac{1}{n}\frac{\partial n}{\partial T} + \alpha$ sets the thermorefractivity and thermal expansion. There are two distinct timescales in this process [13]. The case where α is not used corresponds to the fast thermal relaxation of the WGM volume into an effectively infinite medium of the resonator material. This time scale is defined by thermal relaxation of a WGM volume: $\tau_1 = 1/\delta_\theta$. The case where α is used corresponds to the thermal relaxation of the resonator as a whole and the corresponding timescale may be roughly estimated as $\tau_2 = \frac{R^2}{DNu}$, where Nu is the Nusselt number, ≈0.3 for air [13]. The thermal expansion coefficient α should therefore only be taken into account when analyzing static solutions on timescales in which the resonator will have enough time to thermally expand (i.e., for low or zero laser scan speed). Relaxation of the toroid's temperature through the silicon pillar can also be taken into account. However, the corresponding time constant is usually comparable to that describing the relaxation of the whole resonator. Specifically, the relaxation time constant in the approximation of infinite heat conductance of silicon (it is around two orders of magnitude larger than for silica) is given by:

$$\tau_3 = \frac{\pi R r^2 \ln(R/R_0)}{dD},$$

where R_0 is the radius of the silicon pillar and *d* is the thickness of the silica layer. For a typical silica toroid with *R* = 30μm, R_0 = 3μm, *d* = 4μm, and *r* = 6μm the time constant is τ_3 =

#113430 - $15.00 USD Received 29 Jun 2009; revised 22 Jul 2009; accepted 22 Jul 2009; published 29 Jul 2009

2ms. This value can dramatically decrease if the pillar diameter is comparable to the toroid major diameter.

3. Solution of the nonlinear system and stability analysis

We first consider the static solutions of system (3). To deal with the complex numbers field amplitudes are defined as $a = a_1 + ia_2$ and $b = b_1 + ib_2$; and, upon substitution into (3), we look for the solutions in which a_1, a_2, b_1, b_2 are real. The corresponding system is:

$$\begin{cases} \dot{a}_1 = -a_1\gamma_a + a_2(\omega - \omega_a + \mu_a a^2 + \omega_a\beta_a\theta_a) - kb_2 \\ \dot{a}_2 = -a_2\gamma_a - a_1(\omega - \omega_a + \mu_a a^2 + \omega_a\beta_a\theta_a) + F + kb_1 \\ \dot{b}_1 = -b_1\gamma_b + b_2(\omega - \omega_b + \mu_b b^2 + \omega_b\beta_b\theta_b) - ka_2 \\ \dot{b}_2 = -b_2\gamma_b - b_1(\omega - \omega_b + \mu_b b^2 + \omega_b\beta_b\theta_b) + ka_1 \\ \dot{\theta}_a = -\delta_\theta^a\theta_a + \nu_a\delta_\theta^a a^2 / (\omega_a\beta_a) \\ \dot{\theta}_b = -\delta_\theta^b\theta_b + \nu_b\delta_\theta^b b^2 / (\omega_b\beta_b) \end{cases} . \qquad (4)$$

Here $a^2 = a_1^2 + a_2^2$ and $b^2 = b_1^2 + b_2^2$. This system contains both very large and very small numbers, which creates problems when numerical solvers such as Mathematica or Maple are used. To overcome this difficulty, dimensionless quantities are defined. The following substitutions are made in (4): $a_1 = y_1 a_c,\ a_2 = y_2 a_c,\ b_1 = y_3 b_c,\ b_2 = y_4 b_c,\ t = \tau t_c,\ \theta_a = y_5\theta_c^a,\ \theta_b = y_6\theta_c^b$ and $\Delta\omega_{a,b} = \omega - \omega_{a,b}$ where $a_c = \sqrt{\frac{\gamma_a}{\mu_a}}, b_c = \sqrt{\frac{\gamma_b}{\mu_b}},\ \theta_c^a = \frac{\gamma_a}{\omega_a\beta_a},\ \theta_c^b = \frac{\gamma_b}{\omega_b\beta_b},\ \tau = \frac{1}{\gamma_a}$. With these substitutions, the equations contain only dimensionless values on the order of unity:

$$\begin{cases} \dot{y}_1 = -y_1 + y_2\frac{\Delta\omega_a}{\gamma_a} + y_2y_1^2 + y_2^3 + y_2y_5 - y_4\frac{kb_c}{\gamma_a a_c} \\ \dot{y}_2 = -y_2 - y_1\frac{\Delta\omega_a}{\gamma_a} - y_1^3 - y_1y_2^2 - y_1y_5 + F\sqrt{\frac{\mu_a}{\gamma_a^3}} + y_3\frac{kb_c}{\gamma_a a_c} \\ \dot{y}_3 = -y_3 + y_4\frac{\Delta\omega_b}{\gamma_b} + y_4y_3^2 + y_4^3 + y_4y_6 - y_2\frac{ka_c}{\gamma_b b_c} \\ \dot{y}_4 = -y_4 - y_3\frac{\Delta\omega_b}{\gamma_b} - y_3^3 - y_3y_4^2 - y_3y_6 + y_1\frac{ka_c}{\gamma_b b_c} \\ \dot{y}_5 = -\delta_\theta^a y_5/\gamma_a + \nu_a\delta_\theta^a(y_1^2 + y_2^2)/(\gamma_a\mu_a) \\ \dot{y}_6 = -\delta_\theta^b y_6/\gamma_b + \nu_b\delta_\theta^b(y_1^2 + y_2^2)/(\gamma_b\mu_b) \end{cases} . \qquad (5)$$

We set all time derivatives to zero and find the static solutions of the resulting system using the numerical solver Maple. The power circulating in resonator A, for example, can be estimated as

$$P_{circ} = (y_1^2 + y_2^2)a_c^2\frac{ncV_a}{(2\pi)^2 R_a} \times 10^{-7}[Watt]. \qquad (6)$$

The stability of the static solutions is also considered in a Lyapunov sense. We consider small deviations x_i from the static solutions y_{i0} of system (5) and check that the system tends to return to the static solution. The substitution $y_i = x_i + y_{i0}$, $i = 1..6$ is made in (5) and only contributions linear in x_i are retained to obtain the system $\dot{X} = AX$. The matrix A is:

#113430 - $15.00 USD Received 29 Jun 2009; revised 22 Jul 2009; accepted 22 Jul 2009; published 29 Jul 2009

$$A=\begin{Vmatrix} 2y_{20}y_{10}-1 & \Delta_a+2y_{20}^2 & 0 & -\frac{kb_c}{\gamma_a a_c} & y_{20} & 0 \\ -(\Delta_a+2y_{10}^2) & -(1+2y_{10}y_{20}) & \frac{kb_c}{\gamma_a a_c} & 0 & -y_{10} & 0 \\ 0 & -\frac{ka_c}{\gamma_b b_c} & 2y_{40}y_{30}-1 & \Delta_b+2y_{40} & 0 & y_{40} \\ \frac{ka_c}{\gamma_b b_c} & 0 & -(\Delta_b+2y_{30}^2) & -(1+2y_{40}y_{30}) & 0 & -y_{30} \\ \frac{2\nu_a\delta_\theta^a}{\gamma_a\mu_a}y_{10} & \frac{2\nu_a\delta_\theta^a}{\gamma_a\mu_a}y_{20} & 0 & 0 & -\frac{\delta_\theta^a}{\gamma_a} & 0 \\ 0 & 0 & \frac{2\nu_b\delta_\theta^b}{\gamma_b\mu_b}y_{30} & \frac{2\nu_b\delta_\theta^b}{\gamma_b\mu_b}y_{40} & 0 & -\frac{\delta_\theta^b}{\gamma_b} \end{Vmatrix}$$

. Here $\Delta_a=\frac{\Delta\omega_a}{\gamma_a}+\left(y_{10}^2+y_{20}^2\right)\left(1+\frac{\nu_a}{\mu_a}\right)$ and $\Delta_b=\frac{\Delta\omega_b}{\gamma_b}+\left(y_{30}^2+y_{40}^2\right)\left(1+\frac{\nu_b}{\mu_b}\right)$. We then find a characteristic polynomial of A given by the determinant $det|I\lambda-A|$, where I is a unity matrix. A Routh-Hurwitz criterion is then applied to determine if all the roots of this polynomial have negative real parts, which is a sufficient condition for stability of the static solution y_{i0}.

4. Experimental observation of nonlinear responses

We have studied several silica microtoroid resonator pairs and observed the nonlinear responses under various laser scanning rates and power levels. Figure 2 is a schematic of the experimental setup used for measurements.

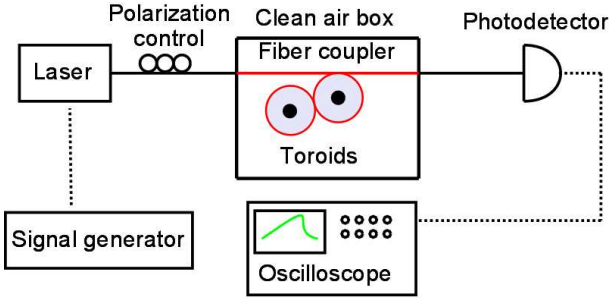

Fig. 2. Schematic of the experimental setup

Individual silica microtoroids were fabricated on the edge of silicon chips using standard techniques [14]. The two, selected toroids having closely aligned optical frequencies were then brought together to enable optical coupling via the evanescent field in the air gap between the resonators. Temperatures of the individual toroids were separately controlled. A New Focus "Velocity" external-cavity, diode laser was used to excite the WG modes. This laser provides up to 6 mW of optical power at the wavelength of 1550 nm and has a linewidth on the order of 0.3 MHz. The laser wavelength could be scanned by applying voltage to the laser head's piezo element. Relative positioning of the microtoroids was controlled with separate nanopositioning stages (PI nanocube). A clean air box was used to preserve the toroids and the coupler in a dust free environment.

In case of a sufficiently low optical pump power, the resonant curve of the bi-resonator system contains two symmetric Lorentzian peaks separated in frequency by double the

#113430 - $15.00 USD Received 29 Jun 2009; revised 22 Jul 2009; accepted 22 Jul 2009; published 29 Jul 2009

coupling constant *k* (see Fig. 3) The splitting of the resonance is a signature behavior of a coupled resonator system.

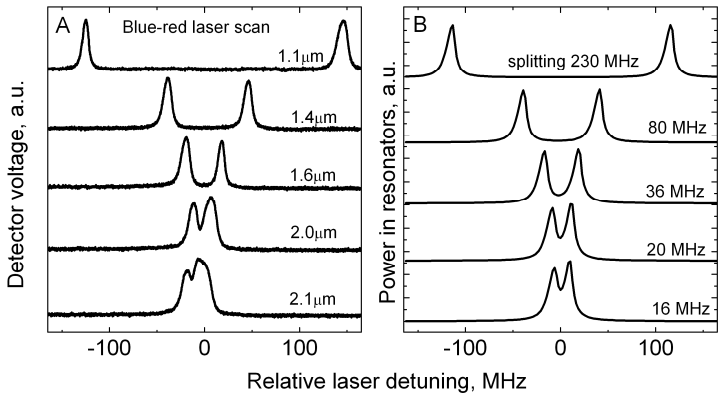

Fig. 3. A: Transmission spectra of coupled resonators recorded for several air gap values. B: Static solutions provided by the model for several values of optical coupling constant. Optical Q used in the model is around 10^7. The asymmetry in the lowest trace was modeled by setting the eigenfrequencies of each resonator slightly mismatched.

Avoided crossing is another typical feature of the coupled resonator system, the appearance of which is caused by the mismatch in the eigenfrequencies of the resonators. An example of this behavior is obtained by changing the temperature of one resonator as shown in Fig. 4. Figure 3 and 4 also demonstrate agreement between the theory and the results of the experiment, validating our model.

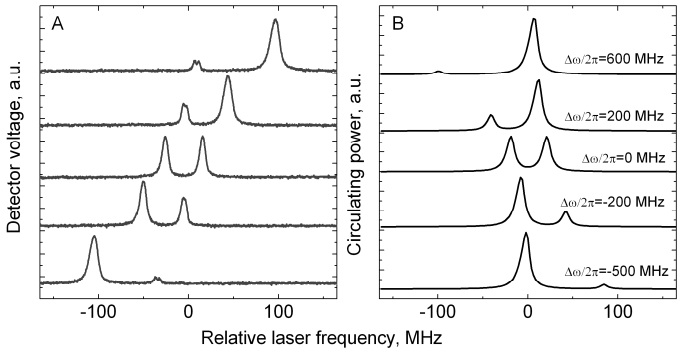

Fig. 4. A: Transmission spectra of coupled resonators recorded as the temperature of one resonator was gradually changing leading to the eigenfrequency shift and avoided crossing. Degenerate splitting is set at 40 MHz. The horizontal shift is due to unintended cross-heating of the resonators by the other resonator's heating element. B: Static solutions obtained theoretically for conditions similar to the experiment.

5. Thermal instability of the compound resonator system

At increased power, we have also observed a nonlinear process in which the thermal effect drives one of the WGM frequencies away from the other, thereby destroying the coupled mode configuration. When this happens, the resulting transmission spectra correspond to a pair of uncoupled microtoroids. To understand how this process takes place it is helpful to monitor the optical power circulating in each resonator. The model is used to approximately fit the experimentally observed resonance curves and to monitor the power in both resonators separately. Two silica microtoroids of major diameters 63μm (A) and 51μm (B) were used for this observation. Resonator A has larger major diameter and smaller pillar, which leads to a larger slow nonlinear susceptibility coefficient.

#113430 - $15.00 USD Received 29 Jun 2009; revised 22 Jul 2009; accepted 22 Jul 2009; published 29 Jul 2009

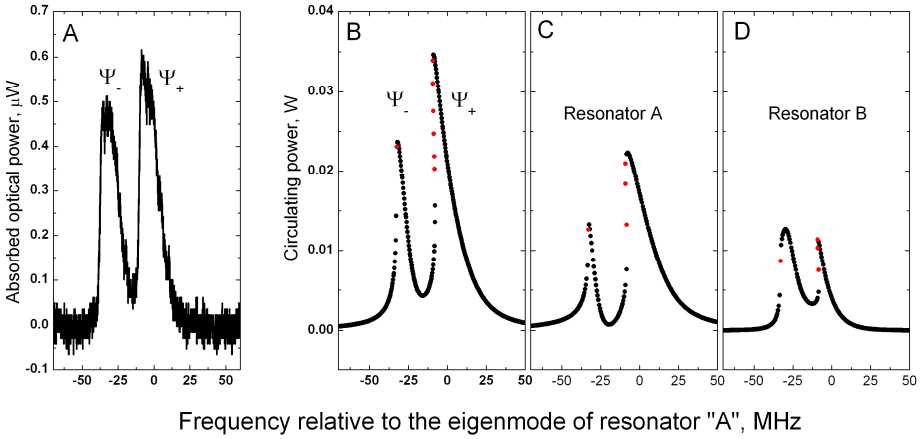

Fig. 5. Experimental transmission spectra and static solutions at low power. Optical pump power is below the nonlinearity threshold and the resulting resonance curve is represented by a double peak. A: transmission spectra from the experiment. B: total optical power circulating in the coupled resonator system. Pump power is 1μW. C: power in resonator A, D: power in resonator B. The partial modes (supermodes) are denoted by Ψ_+ and Ψ_-.

For relatively low optical pump power values that are below the bistability threshold [15], the response of the bi-resonator system is similar to the double Lorentzian of a coupled linear system and is presented on Fig. 5.

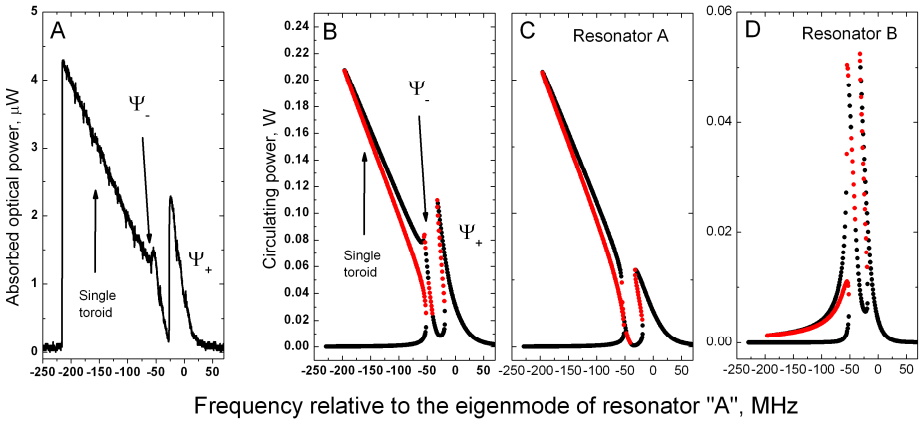

Fig. 6. Experimental transmission spectra and static solutions at moderate power. With further increases in optical pump power (relative to Fig. 5) the red supermode becomes unstable, causing reversion to a transmission spectrum corresponding to a single resonator. A: transmission spectrum from the experiment. B: total optical power circulating in the coupled resonator system. Pump power is 4μW. C: power in resonator A, D: power in resonator B. The partial modes (supermodes) are denoted by Ψ_+ and Ψ_-.

For somewhat higher power, the red supermode becomes unstable for certain laser detuning, and can lead to the set of static solutions that correspond to a single resonator A (i.e., loss of resonance with resonator B), as is shown in Fig. 6. The theoretical model shows (Fig. 6C and 6D) that this process is caused by the difference in the thermal frequency shifts in resonator A and B. While the laser is still exciting the resonator A on its blue, stable side, the resonator B has switched to its unstable, red side of the resonance, and the resonant power transfer to resonator B has ceased. We found that this process has a rather sharp threshold as can be seen in a video in Fig. 8.

#113430 - $15.00 USD Received 29 Jun 2009; revised 22 Jul 2009; accepted 22 Jul 2009; published 29 Jul 2009

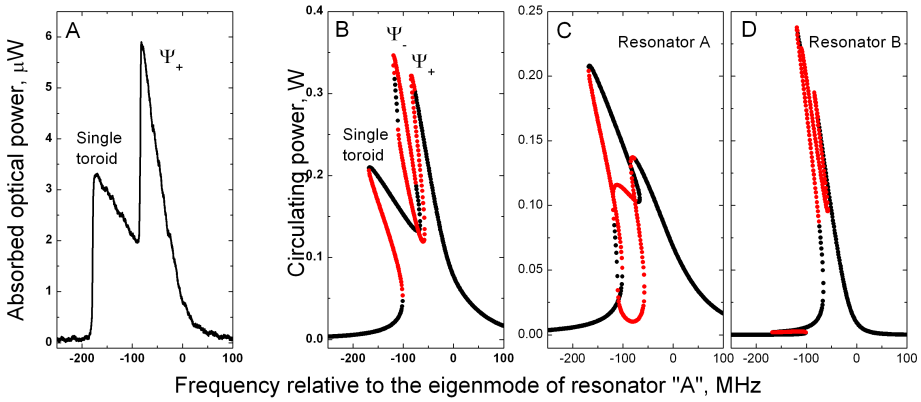

Fig. 7. Experimental transmission spectra and static solutions at high power. Under this condition the red supermode may become unstable and impossible to observe in the experiment. In this particular example the Q factor of resonator A is lower than that of resonator B. A: transmission spectrum from the experiment. B: total optical power circulating in the coupled resonator system. Pump power is 20μW. C: power in resonator A, D: power in resonator B. The partial modes (supermodes) are denoted by Ψ_+ and Ψ_-.

In Fig. 7 we present another state of the bi-resonator system where the red supermode becomes completely unstable and not observable in the experiment. In contrast to Fig. 6, the portion of the transmission spectrum corresponding to a single toroid is now lower than the supermode portion. This is modeled by setting the Q factor of resonator A to be lower than that of resonator B.

It was also found that, depending on the relative Q factor and nonlinear coefficients of the resonators, several instability regimes are possible. If the nonlinear response of the resonator A is stronger, then the response of the system will become identical to the resonator A response after the resonators have been thermally driven out of resonance. This case is presented in Fig. 6. If, however, the response of the resonator B is stronger, then the system will destabilize by shifting the eigenfrequency of the resonator B as long as resonant energy transfer through resonator A is taking place. After the resonance curve of the resonator B reaches its extreme point, the response of the destabilized system will again correspond to that of resonator A. This is a case where four “shark-fin-like” features can appear in the transmission spectrum.

An example of how the transmission spectrum of a system of two identical silica microtoroids evolves as the pump power grows is given in the video in Fig. 8. The parameters used in this video are given in Table 1.

#113430 - $15.00 USD Received 29 Jun 2009; revised 22 Jul 2009; accepted 22 Jul 2009; published 29 Jul 2009

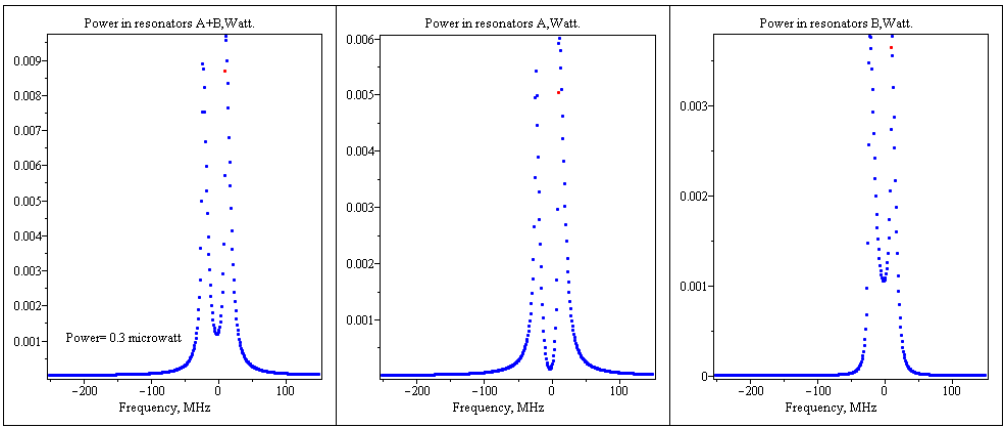

Fig. 8. Nonlinear resonance curve of coupled resonator system for increasing pump power values. Note the sharp transition around 0.9μW pump power (Media 1)

Table 1. Parameters used in computation of resonance curve in Fig. 8.

Parameter	Value
Optical quality factor, Q	2×10^7
Density, ρ	2.2 g/cm^3
Thermal diffusivity, D	9.5×10^{-3} cm^2/s
Heat capacity, C	6.7×10^6 erg/(gK)
Effective third order susceptibility, $\chi^{(3)}$	1.7×10^{-10} cm^3/erg
Absorption coefficient, α	5×10^{-6} cm^{-1}
Thermal expansion and thermorefractivity, β	8.83×10^{-6} K^{-1}
Refractive index, n	1.46
Laser wavelength, λ	1550 nm
Toroid major radius, R	30 μm

Finally, the instability behavior is not always experimentally observable as the destabilized island of static solutions may be separated from the split Lorentzian by a region of unstable solutions.

6. Discussion

Since a system of two cubic differential equations may have up to nine static solutions for each value of the independent variable (laser detuning in our case), several types of qualitatively different transmission spectra are possible at high power. These include the standard "shark fin" spectrum for a single resonator, "double shark fin" for a coupled linear resonators similar to that of Fig. 3-4, and "triple shark fin" as shown on Fig. 6. Solutions with four "shark fins" are also possible from our model, however not all "fins" will be stable and thus not observable in the experiment. It is also found that the form of the static solutions is sensitive to input conditions. Given the lengthy computational time we did not attempt to run the automated parameter fitting. Thus our results do not match the experimental data precisely. We believe that any experimental situation can be appropriately modeled with our equations. However, the equations should be used with care when the experimental conditions lead to more than one time constant in the involved thermal processes. This can happen, for example, when the blue supermode experiences a bistable transition to the set of solutions having lower power and the temperature of the resonator begins to adjust. Access to regimes in which the thermal time constant or relaxation mechanism change is possible by adjustment of the laser scan rate. In the present work the scan rate has been accordingly adjusted so that

#113430 - $15.00 USD Received 29 Jun 2009; revised 22 Jul 2009; accepted 22 Jul 2009; published 29 Jul 2009

primarily the fast thermal time constant is studied. As the effective nonlinearity depends on laser scan rate [13], we use the effective $\chi^{(3)}$ as a fitting parameter.

As coupled resonator systems find new applications it is important to understand the nonlinear effects that govern static and dynamic behavior in such systems. The model presented here can be used to describe nonlinear behavior of the coupled whispering gallery mode resonator systems over a wide variety of experimental parameters. The model can be generalized to other coupled oscillator systems.

Acknowledgments

We would like to acknowledge the support from DARPA. ISG thanks A. B. Matsko, M. L. Gorodetsky, A. E. Fomin and Tao Lu for helpful discussions.

#113430 - $15.00 USD Received 29 Jun 2009; revised 22 Jul 2009; accepted 22 Jul 2009; published 29 Jul 2009